Mutational Analysis of Peptidyl Carrier Protein and Acyl Carrier Protein Synthase Unveils Residues Involved in Protein−Protein Recognition †

3 **AUTHORS**, INCLUDING:

Mohammad Mofid
Isfahan University of Medical Sciences
47 PUBLICATIONS **830** CITATIONS

SEE PROFILE

Mutational Analysis of Peptidyl Carrier Protein and Acyl Carrier Protein Synthase Unveils Residues Involved in Protein−Protein Recognition[†]

Robert Finking,[‡] Mohammad Reza Mofid, and Mohamed A. Marahiel*

Philipps-Universität Marburg, Fachbereich Chemie/Biochemie, Hans-Meerwein-Strasse, D-35032 Marburg, Germany

Received February 11, 2004; Revised Manuscript Received April 27, 2004

ABSTRACT: 4′-Phosphopantetheinyl transferases (PPTases) are essential for the production of fatty acids by fatty acid synthases (primary metabolism) and natural products by nonribosomal peptide synthetases and polyketide synthases (secondary metabolism). These systems contain carrier proteins (CPs) for the covalent binding of reaction intermediates during synthesis. PPTases transfer the 4′-phosphopantetheine moiety from coenzyme A (CoA) onto conserved serine residues of the apo-CPs to convert them to their functionally active holo form. In bacteria, two types of PPTases exist that are evolutionary related but differ in their substrate spectrum. Acyl carrier protein synthases (AcpSs) recognize CPs from primary metabolism, whereas Sfp- (surfactin production-) type PPTases have a preference for CPs of secondary metabolism. Previous investigations showed that a peptidyl carrier protein (PCP) of secondary metabolism can be altered to serve as substrate for AcpS. We demonstrate here that a single mutation in PCP suffices for the modification of this CP by AcpS, and we have identified by mutational analysis several other PCP residues and two AcpS residues involved in substrate discrimination by this PPTase. These altered PCPs were still capable of serving their designated function in NRPS modules, and selective use of AcpS or Sfp leads to production of two different products by a trimodular NRPS.

A large and diverse number of natural products and fatty acids are produced on protein templates of modularly organized megaenzymes such as nonribosomal peptide synthetases (NRPSs),[1] polyketide synthases (PKSs), and fatty acid synthases (*1−4*). Although they are diverse in their biosynthetic strategies, common to all these systems is a small (10 kDa) protein or protein domain that acts as the transport unit of intermediates during synthesis. These so-called 4′-phosphopantetheine- (4′PP-) dependent carrier proteins (CPs) are part of a superfamily whose members have names that reflect their designated substrate (*5, 6*). Acyl carrier proteins (ACPs) are part of fatty acid and polyketide synthases, whereas aryl (ArCPs) and peptidyl carrier proteins (PCPs) (amino acyl or peptidyl substrates) are used by NRPSs. The CPs can be further subdivided according to their affiliation with primary (fatty acid, membrane assembly) and secondary (NRPS, PKS) metabolism. However, although CPs play a decisive role in the synthesis of a variety of products,

crystallographic studies have revealed a common four-helix bundle fold (*7−12*). The structure of the CP exhibits a certain flexibility, which allows adaptation to the different interacting proteins (*6, 11, 13, 14*). In addition, protein−protein interaction and discrimination is thought to be mediated by helix 2 of the CP, which was deduced from the cocrystal structure of ACP, acyl carrier protein synthase (AcpS) (*8*), *Escherichia coli* β-ketoacyl-ACP synthase III-ACP docking (*15*), and a mixed ACP/PCP hybrid protein (*6*). Additionally it was shown that a PCP's helix 2 shows obvious differences depending on the localization within the modular architecture, which is in accordance with the enzymes that represent the interacting protein partners (*5, 6*).

As an essential requirement for the activity of the CP, it must interact with a 4′-phosphopantetheinyl transferase (PPTase) that posttranslationally modifies the inactive apo-CP. Activation of the CP proceeds via Mg^{2+}-dependent 4′-PP transfer from CoA onto a conserved serine residue of the CP catalyzed by the PPTase, which leaves the CP in the active state, referred to as holo-CP (Figure 1) (*16*). The 4′-PP moiety has a terminal sulfhydryl group that is subsequently used to bind intermediates as energy-rich thioesters during product assembly. In bacteria, two types of PPTases are known (*16*), the AcpS type of primary metabolism and the Sfp type of secondary metabolism. The two types of PPTases can be distinguished by their size, oligomeric state, and substrate selectivity. AcpS-type PPTases are homotrimers of 120−140 residue protomers that activate solely CPs of primary metabolism (*6, 8, 17−20*). Sfp-type PPTases, on the other hand, have been shown to be promiscuous. These ca. 240 residue pseudohomodimers (*21, 22*) are thought to be dedicated to secondary metabolism if a second, AcpS-
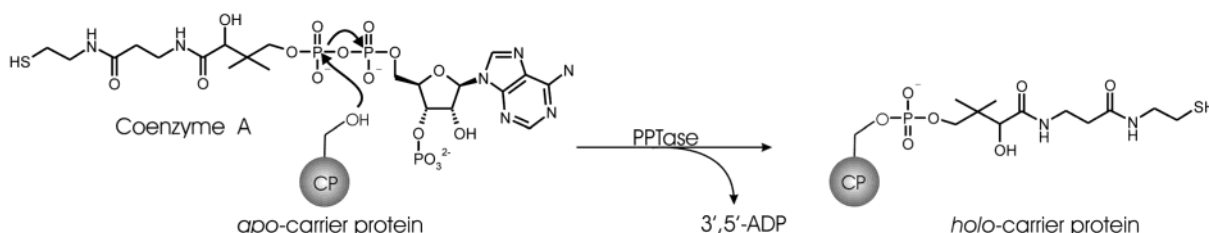
FIGURE 1: PPTases transfer the 4′-phosphopantetheine moiety from CoA on a conserved serine residue of the apo carrier protein, which is thus converted into its active holo form.
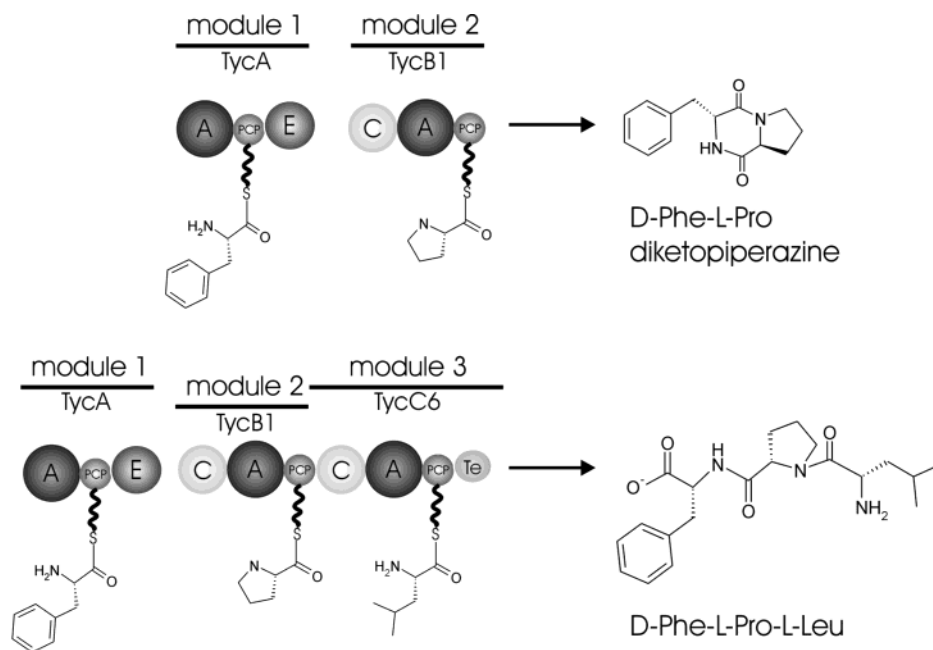

FIGURE 2: Domain structure of the nonribosomal peptide synthetases TycA, TycB1, and TycB1−TycC6; abbreviations are A, adenylation domain; PCP, peptidyl carrier protein domain; E, epimerization domain; C, condensation domain; and Te, thioesterase domain. A combination of TycA and TycB1 can be used to produce D-Phe-L-Pro-diketopiperazine (DKP), while TycA and the fused modules TycB1−TycC6 are used as a model system for the production of D-Phe-L-Pro-L-Leu (FPL).

type PPTase is present in the organism, although they accept CPs of both primary and secondary metabolism as substrates with clear preference for those of secondary metabolism in vitro (19, 23, 24). In bacteria that lack a PPTase of primary metabolism, the Sfp-type PPTase seems to have been evolutionarily selected for high efficiency with CPs of primary metabolism, although the enzymes maintain broad substrate tolerance (25, 26).

Although a previous study has revealed that helix 2 of the CP is used by PPTases as the distinguishing element, individual recognition sites of the CP have remained elusive (6). To address this question, we have constructed several PCP mutants that were tested for positive interaction with both *Bacillus subtilis* AcpS and Sfp. As we will show, a single mutation suffices to allow recognition by AcpS, that does not modify the wild-type PCP. In addition we have tested these PCP mutants in the context of a module and found them still capable of participation in nonribosomal peptide synthesis. For this purpose, we have made use of a model system composed of TycA in combination with either TycB1, for the production of D-Phe-L-Pro diketopiperazine (DKP), or TycB1-TycC6-Te, for the production of the tripeptide D-Phe-L-Pro-L-Leu (FPL) (Figure 2). The TycA initiation module comprises an adenylation (A) domain for amino acid activation as well as a PCP domain that acts as the carrier of the activated amino acid and an epimerization

(E) domain for the epimerization of the substrate amino acid. TycB1 is a module composed of a condensation (C) domain that is responsible for peptide bond formation, an A domain that activates Pro, and a PCP domain [also referred to as thiolation (T) domain]. TycB1 is therefore referred to as ProCAT to indicate the domain structure and the selectivity of the A-domain. Consequently, TycC6 is referred to as LeuCAT. The Te domain is fused to the trimodular TycB1-TycC6-Te (ProCAT-LeuCAT-Te) because it catalyzes product release of the tripeptide.

We have previously used a superposition of Sfp and AcpS to identify equivalent residues of the two PPTases Sfp and AcpS from *B. subtilis* involved in the CP recognition (27). On the basis of this analysis we have now generated AcpS mutants with the aim of further substantiating the evolutionary relatedness of the two enzymes. The mutants were generated such that they make AcpS more Sfp-like; however, none of the mutants was capable of recognizing the wild-type PCP, although the mutated residues are clearly involved in CP interaction.

EXPERIMENTAL PROCEDURES

Unless otherwise specified, standard protocols were used (28). *E. coli* was grown on LB medium. Wherever necessary, antibiotics were added to the medium at the following

Table 1: Oligonucleotides Used for Site-Directed Mutagenesis

comment	oligonucleotides 5′–3′	template	method
a	(1) CGCTGGGCGGCGATTCGTTAGACGCGATTGAGCTCATTTCC (2) GGAAATGAGCTCAATCGCGTCTAACGAATCGCCGCCCAGCG	pQE60[*ProCAT*], pQE60[*ProCAT-LeuCAT-Te*]	B
b	(1) GCTCATTTCCCGCATCGAAGACGAATGCCAGGCGGATG (2) CATCCGCCTGGCATTCGTCTTCGATGCGGGAAATGAGC	pQE60[*ProCAT*], pQE60[*ProCAT-LeuCAT-Te*]	A
c	(1) GCTCATTTCCCGCATCGAAGACGAATGCCAGGCGGATG (2) CATCCGCCTGGCATTCGTCTTCGATGCGGGAAATGAGC	pQE60[*ProCAT-V1*], pQE60[*ProCAT-V1-LeuCAT-Te*]	A
K47A	(1) GCGGACATTCCTTGGCAGCCATGGCTGTCGCTGCAC (2) GTGCAGCGACAGCCATGGCTGCCAAGGAATGTCCGC	pQE60[*TycC3 PCP*]	B
K47D	(1) GCGGACATTCCTTGGCAGCCATGGCGTGTCGCTGCAC (2) GTGCAGCGACAGCCATGGCGTCCAAGGAATGTCCGC	pQE60[*TycC3 PCP*]	B
R14A	(1) TGGACATTACCGAGCTTAAAGCCATCGCCTCTATGGCTGGGC (2) GCCCAGCCATAGAGGCGATGGCTT TAAGCTCGGTAATGTCCA	pTz18R[*acpS*]	A
K44A	(1) GACCAATACTATGAGCTTTCAGAGGCCAGAAAAAACGAATTTCTCGC (2) GCGAGAAATTCGTTTTTTCTGGCCTCTGAAAGCTCATAGTATTGGTC	pTz18R[*acpS*]	A
R14K	(1) TGGACATTACCGAGCTTAAAAAGATCGCCTCTATGGCTGGGC (2) GCCCAGCCATAGAGGCGATCTTTTTAAGCTCGGTAATGTCCA	pTz18R[*acpS*]	A
K44D	(1) GACCAATACTATGAGCTTTCAGAGGATCGAAAAAACGAATTTCTCGCGGG (2) CCCGCGAGAAATTCGTTTTTTCGATCCTCTGAAAGCTCATAGTATTGGTC	pTz18R[*acpS*]	A
R14K, K44D	(1) TGGACATTACCGAGCTTAAAAAGATCGCCTCTATGGCTGGGC (2) GCCCAGCCATAGAGGCGATCTTTTTAAGCTCGGTAATGTCCA	pTz18R[*acpS K44D*]	A

a ProCAT-V1 and ProCAT-V1-LeuC AT-Te. *b* ProCAT-V2 and ProCAT-V2- LeuCAT-Te. *c* ProCAT-V3 and ProCAT-V3- LeuCAT-Te.

concentrations: ampicillin, 100 μg/mL, kanamycin, 25 μg/mL. Oligonucleotides for PCR and site-directed mutagenesis were purchased from Qiagen-Operon (Cologne, Germany). ^{3}H-Labeled CoA was purchased from Hartmann Analytics (Braunschweig, Germany).

Mutagenesis of the acpS, tycC3-PCP, and ProCAT Genes. Mutations in the *acpS*, *tycC3-PCP*, *ProCAT*, and *ProCAT-LeuCAT-Te* genes were introduced by one of two methods (Table 1):

(Method A) Mutations in the *acpS*, *tycC3-PCP*, *ProCAT*, and *ProCAT-LeuCAT-Te* genes were introduced by use of the QuickChange kit (Stratagene, Heidelberg, Germany) according to the manufacturer's recommendations. For this purpose, two primers were used in a PCR with either pTz18R[*acpS*] (*19*), pQE60[*ProCAT*] (*29*), pQE60[*ProCAT-LeuCAT-Te*] (TycB1-TycC6-Te) (*29*), pQE60[*ProCAT-V1-LeuCAT-Te*], or pQE60[*ProCAT-V1*] as template and *Pfu*-Turbo DNA polymerase (Stratagene, Heidelberg, Germany). Both primers contained the desired mutation and annealed to the same sequence on opposite strands. Thus, the whole plasmid was amplified. Following PCR, *Dpn*I was added to the PCR mixture and the template was digested for 1 h at 37 °C. XL1-Blue competent cells (Stratagene, Heidelberg, Germany) were subsequently transformed with the digested PCR mixture.

(Method B) Mutations in the *PCP* gene and one mutation in the *ProCAT* and *ProCAT-LeuCAT-Te* genes were introduced by inverse PCR with pQE70[*tycC3-PCP*] (*9*) or pQE60[*ProCAT*] (*29*) as template. For this purpose, oligunucleotides were used that contained the desired mutation in addition to an extra restriction site for the subsequent religation of the two ends generated by PCR. For PCR, either *Vent*- or *Herculase*-Hotstart DNA polymerase (NEB, Schwalbach, Germany) was used. The generated PCR fragments were purified, digested with *Dpn*I and the appropriate restriction enzyme, and subsequently religated. XL1-Blue competent cells (Stratagene, Heidelberg, Germany) were thereafter transformed with the ligation mixture.

All constructs generated by either of the two methods were sequenced prior to heterologous expression in *E. coli*. Sequences of all primers used can be found in Table 1.

Overproduction and Purification of Recombinant Proteins. *E. coli* BL21(λDE3) (Merck Biosciences, Schwalbach, Germany) was transformed with the mutants generated by the above-mentioned methods for the production of the PCP-His$_6$, ProCAT-His$_6$, and ProCAT-LeuCAT-Te-His$_6$ fusion protein mutants. A portion (5 mL) of an overnight culture of each strain in LB was inoculated into 500 mL of the same medium. Expression was induced by addition of 0.1 mM IPTG (final concentration) at an A_{600} of 0.6–0.7 and the culture was allowed to grow for an additional 2 h before being harvested by centrifugation at 4500g and 4 °C. The cells were resuspended in buffer A [50 mM Hepes and 300 mM NaCl (pH 7.8)] and disrupted by three passages through a cooled French pressure cell. The resulting crude extract was centrifuged at 36000g at 4 °C for 30 min. Protein purification by Ni^{2+}-affinity chromatography was carried out as previously described (*6*). Those fractions containing the desired protein were pooled, brought to 10% glycerol (v/v), and stored at −80 °C.

In the case of the *acpS* mutants, the culture was grown at 37 °C and 300 rpm until an A_{600} of 0.5–0.7 was reached. Expression was induced by addition of 1 mM IPTG (final concentration) and the culture was allowed to grow for an additional 3–5 h before being harvested by centrifugation at 4500g and 4 °C. The cells were resuspended in buffer GFC1 [50 mM NaH$_2$PO$_4$/Na$_2$HPO$_4$ and 20% (v/v) glycerol (pH 7.0)] and disrupted by three passages through a cooled French pressure cell. The resulting crude extract was centrifuged at 36000g at 4 °C for 30 min and subsequently applied to a Superdex 75 26/60 gel-filtration column (Amersham Biosciences, Uppsala, Sweden) equilibrated with GFC1. Isocratic elution was performed with GFC1 at 1 mL/min, and 4 mL fractions were taken. Those fractions containing the desired AcpS mutant were pooled and applied to a 6 mL Resource15S ion-exchange column (Amersham Biosciences, Uppsala, Sweden) that had been equilibrated with GFC1 at 5 mL/min. After the column had been washed with 30 mL of GFC1 to wash off unbound proteins, a 120 mL linear gradient to 100% buffer CEX [50 mM NaH$_2$PO$_4$/Na$_2$HPO$_4$ and 500 mM NaCl (pH 7.0)0 was applied at 5 mL/min, and 2 mL fractions were taken. The fractions that

contained the desired protein were pooled and concentrated by use of Vivaspin (Vivascience AG, Hannover, Germany) with a molecular weight cutoff of 10 000. The concentrated protein solution was applied to a Superdex75 16/60 (Amersham Biosciences, Uppsala, Sweden) that had been equilibrated with buffer GFC2 [50 mM Tris/HCl and 20% glycerol (pH 8.8)]. Isocratic elution was performed with GFC2 at 1 mL/min, and 2 mL fractions were taken. Those fractions containing the AcpS mutant were pooled and stored at −80 °C.

The presence of the respective proteins in the fractions was detected by SDS−polyacrylamide gel electrophoresis analysis (15% Laemmli gels). TycC3-PCP, AcpS from *B. subtilis*, Sfp of *B. subtilis*, and ACP from *B. subtilis*— hereafter referred to as PCP, AcpS, Sfp, and ACP, respectively—as well as hTycA were produced and purified as previously described (*6*, *19*). Wild-type ProCAT-LeuCAT-Te was obtained as described by Mootz and co-workers (*29*). Protein concentrations were determined on the basis of the calculated extinction coefficient at 280 nm: all AcpS mutants, 6520 M^{-1} cm^{-1}; ProCAT-V1−3, 92 230 M^{-1} cm^{-1}; PCP mutants, 9530 M^{-1} cm^{-1}; ProCAT-V1−3-LeuCAT-Te, 212 480 M^{-1} cm^{-1}.

Radioassay for the Detection of Posttranslational Modification Activity (Priming Assay). The activity of Sfp and AcpS (including the mutants generated) was tested by a method that measures the incorporation of ^{3}H-labeled 4′-phosphopantetheine from [^{3}H]CoA into apo-CPs essentially as described earlier (*6*). Reaction mixtures (100 μL, in duplicate) containing 50 mM Tris/HCl (pH 8.8) [75 mM MES/HCl and 250 mM NaCl (pH 6.0) in the case of Sfp], 10−12 mM $MgCl_2$, 90−100 μM ACP, PCP, or hPCP (*6*), 20−100 μM CoA, 200 nM−20 μM [^{3}H]CoA (specific activity 40 Ci/mmol, 0.95 mCi/mL), and 25 nM−1 μM AcpS or Sfp or 1 μM AcpS mutants were incubated at 37 °C for 30 min (18 h in the case of the AcpS mutants). Reactions were stopped by the addition of 0.8 mL of ice-cold 10% TCA (w/v) and 15 μL of BSA (25 mg/mL). Precipitated protein was collected by centrifugation at 13 000 rpm and 4 °C for 15 min in a tabletop centrifuge. The pellet was washed twice with 0.8 mL of ice-cold TCA (w/v) and resuspended in 180 μL of formic acid. The resulting suspension was mixed with 3.5 mL of Rotiszint Eco Plus scintillation fluid (Roth, Karlsruhe, Germany) and counted in a 1900CA Tri-Carb liquid scintillation analyzer (Packard, Dreieich, Germany).

Kinetic Analysis. For kinetic studies, the amount of holo-carrier protein formed was determined by an HPLC method essentially as described previously (*19*, *25*).

(A) Reaction mixtures (100 μL) contained the apo-carrier protein (1−125 μM PCP, hPCP, PCP-K47A, or PCP-K47D), 25 nM PPTase, 75 mM MES/HCl (pH 6.0) [in the case of AcpS, 50 mM Tris/HCl (pH 8.0)], 250 mM NaCl, 100 μM DTT, 10 mM $MgCl_2$, and 100 μM CoA. The reaction was started by addition of the PPTase and allowed to proceed for 30 min at 37 °C before the addition of 140 μL of acetonitrile to terminate the reaction. The mixtures were centrifuged at 16000*g* for 10 min at RT in a tabletop centrifuge. An aliquot (100 μL) of the clear supernatant was subsequently injected onto an analytical reversed-phase HPLC column (Nucleosil C18, 250 mm, 5 μm, 300 Å, Macherey & Nagel, Germany) that had been equilibrated with 60% solvent A (0.05% trifluoroacetic acid). Absorbance

at 220 nm was monitored. Apo- and holo-CP could be separated by applying a 13.5 mL linear gradient to 57.3% solvent B (acetonitrile in 0.05% trifluoroacetic acid) followed by a 0.9 mL linear gradient to 95% solvent B (flow rate 0.9 mL/min and temperature 45 °C). Under these conditions, the apo-CP migrates faster than the holo-CP. Retention times of the holo-CP and apo-CP were as follows: PCP (11.3 and 13.1 min), hPCP (26.1 and 27.7 min), PCP-K47A (11.1 and 12.6 min), and PCP-K47D (11.3 and 13.3 min).

(B) Reaction mixtures (800 μL) contained the apo-carrier protein (2−235 μM ACP), 50 mM Tris/HCl (pH 8.8), 10 mM $MgCl_2$, and 500 μM CoA. The reaction was started by the addition of AcpS to a final concentration of 4.9−507.5 nM; reaction mixtures were incubated at 37 °C for 5−30 min. The reaction was stopped and the protein was precipitated by the addition of 10% TCA (final concentration). Precipitated protein was collected by centrifugation at 13 000 rpm and 4 °C for 30 min in a microcentrifuge. The pellet was resuspended in 120 μL of 50 mM Tris/HCl, pH 8.8. A 10−100 μL sample of this solution was injected onto an analytical reversed-phase HPLC column (Nucleosil C18, 250 mm, 5 μm, 300 Å, Macherey & Nagel, Germany) that had been equilibrated with 5% solvent C (0.1% trifluoroacetic acid). Absorbance at 220 nm was monitored. Apo- and holo-ACP could be separated by applying a 24.4 mL linear gradient to 70% solvent D (acetonitrile in 0.1% trifluoroacetic acid) followed by a 2.7 mL linear gradient to 95% solvent D (flow rate 0.9 mL/min and temperature 45 °C). Under these conditions, holo-ACP migrates faster than apo-ACP (21.02 and 21.76 min, respectively). The amount of holo-ACP formed was determined by comparing the peak area of the holo-ACP formed with those of both apo- and holo-ACP and subtracting the amount of holo-ACP that was already present after the heterologous expression of the protein in *E. coli* (see Results).

Kinetic constants were determined by a Michaelis−Menten fit of the data sets derived from the HPLC methods (PPTase rate vs substrate concentration). The kinetic constants of the ProCAT mutants were determined by a radioassay method as described previously (*24*).

DKP Assay. The DKP assay is based on a method described by Linne and Marahiel with modifications (*30*). Reaction mixtures (100 μL) contained 1.25 μM ProCAT or its mutants (ProCAT-V1−3), 50 nM PheATE, 2.5 mM L- or D-Phe, 2.5 mM L-Pro, 25 nM AcpS or Sfp, 200 μM CoA, and condensation buffer [50 mM Tris/HCl, 5 mM DTT, 10 mM $MgCl_2$, 250 mM NaCl (pH 8.0)]. The reaction mixtures were preincubated for 15 min at 37 °C and the reaction was started by the addition of 10 mM ATP (final concentration). The reaction was allowed to proceed for a specific time at 37 °C before it was terminated by addition of 0.4 mL butanol/chloroform (4:1 v/v). Water (200 μL) was subsequently added and the mixture was vortexed for 20 s to extract the DKP. The phases were separated by centrifugation at 16000*g* for 2 min. The organic phase was transferred to a fresh reaction cup and the aqueous phase was extracted a second time with 0.4 mL butanol/chloroform (4:1 v/v). The organic phases were combined and washed twice with 0.3 mL of water. The organic solvents were subsequently evaporated and the resulting pellet was dissolved in 50 μL of 10% methanol and 0.05% (v/v) formic acid. A 50 μL portion of a 70:30 mixture of solvent E [0.05% (v/v) formic acid] and
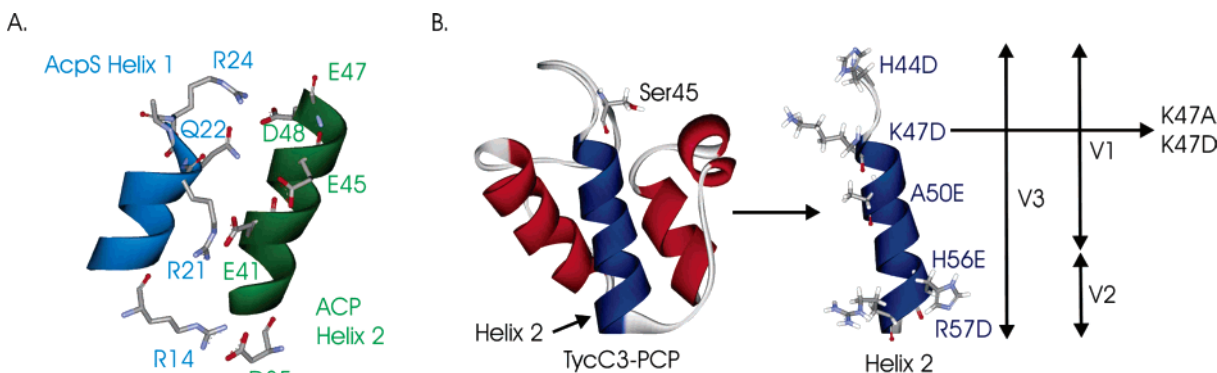
FIGURE 3: (A) Detailed view of the interaction between ACP and AcpS. Interacting residues are found in helix 1 of AcpS and helix 2 of the CP. (B) Construction of the PCP mutants. Shown is the TycC3-PCP structure and helix 2 in detail. Mutant V1 contains mutations H44D, K47D, and A50E; mutant V2 contains mutations H56E and R57D; and mutant V3 contains all of these mutations. Two additional PCP mutants were constructed whose residue 47 was mutated either to Ala or Asp. The vertical arrows indicate the residues that were mutated in V1, V2, and V3, whereas the horizontal arrow points to residue that was mutated in PCP-K47A and -K47D.

solvent F [0.05% (v/v) formic acid in methanol] was added, and 30 μL of this mixture was injected on an analytical (C_{18}) HPLC column (Grom-Sil 120-ODS-4-HE 3 mm × 60 mm, GROM Herrenberg, Germany) that had been equilibrated with 10% solvent F/90% solvent E. Absorbance at 214 nm was monitored. The DKP isoforms D,L-DKP and L,L-DKP were separated through isocratic elution with 25% solvent F/75% solvent E at 1.0 mL/min and temperature 23 °C. The respective elution times were 5.5 min (D,L-DKP) and 6.5 min (L,L-DKP).

Tripeptide Assay. Detection of the tripeptide D-Phe-L-Pro-L-Leu was carried out according to a previously described method (*29*). Reaction mixtures (100 μL) contained 50 nM TycA or hTycA, 1.25 μM ProCAT-LeuCAT-Te or the mutants thereof, 2.5 mM L- or D-Phe, L-Pro, L-Leu, 25 nM PPTase (AcpS or Sfp), 200 μM CoA, and condensation buffer. The mixtures were preincubated for 15 min at 37 °C before 10 mM ATP was added to start the reaction. Samples were taken at defined time points and the reaction was stopped by addition of 0.4 mL of butanol/chloroform 4:1 (v/v). Extraction of the tripeptide was performed as described for DKP (see above).

RESULTS

Overproduction and Purification of the PCP and AcpS mutants. The PCP mutants K47A and K47D, TycA (Pro-CAT) as well as the TycA-TycC6-Te (ProCAT-LeuCAT-Te) mutants V1−3 and PCP-K47A and -K47D were produced as C-terminal His6-tag fusion proteins and purified by Ni^{2+}−NTA affinity chromatography. AcpS mutants were produced untagged and were purified by gel-filtration and ion-exchange chromatography (see Experimental Procedures). The yield per liter of cell culture was 7 mg of the ProCAT and ProCAT-LeuCAT-Te mutants V1−3, 2 mg of the PCP mutants K47A and K47D, 3 mg of the ProCAT mutants K47A and K47D, and 1.8−2 mg of the AcpS mutants. All proteins had a purity of >90% as judged by SDS−PAGE. *B. subtilis* Sfp and AcpS, ACP, hPCP, PCP, TycA, hTycA, ProCAT-LeuCAT-Te, and ProCAT were produced and purified as described previously (*6, 19, 29*). The ratios of apo- to holo-CP as determined by either HPLC method A or B or the loading assay were as follows: ACP, 77:13; PCP, 7:93; hPCP, 21:79; ProCAT, ProCAT-LeuCAT-Te, ProCAT-V2, and ProCAT-V2-LeuCAT-Te, 1:99; PCP-

K47A, 34:66; PCP-K47D, 51:49; ProCAT-V1 and ProCAT-V1-LeuCAT-Te, 12:88; and ProCAT-V3 and ProCAT-V3-LeuCAT-Te, 70:30.

Adaptation of PCP for Posttranslational Modification with AcpS. Previous investigations revealed that PCP can be adapted for the modification with AcpS. This was achieved by an exchange of 14 amino acids in helix 2 of PCP with the corresponding residues from ACP, which yielded a new CP, the hPCP (*6*). This, however, is a rather drastic method and does not unveil the individual residues involved in the interaction with the PPTase. Data from the AcpS−ACP cocrystal pointed to interactions between five acidic residues in helix 2 of ACP (D35, E41, E45, D48, and E47) and four mostly basic residues of AcpS (R14, R21, Q22, and R24; Figure 3A) (*8*). Sequence comparison of ACPs and PCPs upstream of C-domains (PCP^{C}s) (*5, 6*) shows conservation of these residues among ACPs. To unravel the selectivity-conferring residues of ACP with respect to the interaction with a PPTase, we have constructed five ProCAT mutants and two PCP mutants, all of which contain mutations in helix 2 of the PCP domain to convert the PCP stepwise to a CP that comes close to the hPCP. Mutant ProCAT-V1 contains the mutations H44D, K47D, and A50E, whereas mutant ProCAT-V2 contains two point mutations, H56E and R57D, and mutant ProCAT-V3 has all five mutations, namely, H44D, K47D, A50E, H56E, and R57D (Figure 3B). In addition to the monomodular ProCAT, the dimodular Pro-CAT-LeuCAT-Te (TycB1-TycC6-Te) was also equipped with the ProCAT mutants V1−3, which yielded three mutant dimodular proteins.

The priming assay with ^{3}H-labeled CoA showed that the wild-type ProCAT's as well as ProCAT-V2's PCP domain is only modified by Sfp, whereas the PCP of mutants V1 and V3 are modified by Sfp and AcpS alike, which is independent of whether the mutant PCPs are integrated in mono- or dimodular systems (Figure 4). This prompted us to investigate the catalytic constants of the modification with AcpS and Sfp. For this purpose, the concentration of the proteins was varied from 1 to 100 μM. Michaelis−Menten constants, which can be found in Table 2, were determined by HPLC method A through a Michaelis−Menten fit of the data sets. The catalytic constants of AcpS show that an increase in catalytic efficiency correlates with an increased number of mutations that are supposed to make the protein
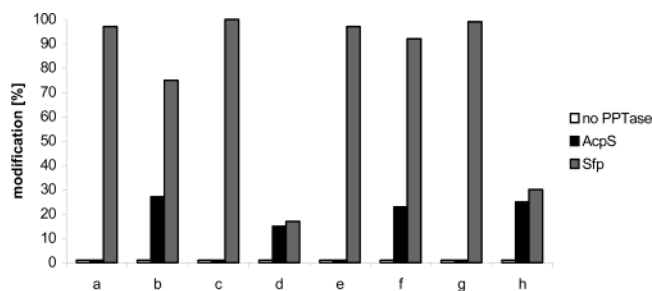
FIGURE 4: Posttranslational modification of the ProCAT mutants in the ProCAT and ProCAT-LeuCAT-Te constructs by AcpS and Sfp in vitro. AcpS or Sfp (25 nM) was incubated with 20 μM CoA, 200 nM [^{3}H]-CoA, and 10 mM MgCl$_2$ for 30 min at 37 °C. (a) Wild-type ProCAT (control); (b) ProCAT-V1; (c) ProCAT-V2; (d) ProCAT-V3; (e) wild-type ProCAT-LeuCAT-Te (control); (f) ProCAT-V1-LeuCAT-Te; (g) ProCAT-V2-LeuCAT-Te; (h) Pro-CAT-V3-LeuCAT-Te. Whereas ProCAT-V2 and ProCAT-V2-LeuCAT-Te were modified by Sfp only, ProCAT-V1, ProCAT-V3, ProCAT-V1-LeuCAT-Te, and ProCAT-V3-LeuCAT-Te were modified by AcpS and Sfp alike. The wild-type proteins were only modified by Sfp, as expected.

Table 2: Kinetic Constants and Efficiencies of AcpS and Sfp with PCP Mutants

substrate	K_m (μM) AcpS	K_m (μM) Sfp	k_{cat} (min^{-1}) AcpS	k_{cat} (min^{-1}) Sfp	k_{cat}/K_m (min^{-1} μM^{-1}) AcpS	k_{cat}/K_m (min^{-1} μM^{-1}) Sfp
ProCAT	nd[a]	2.1 ± 1	nd	55 ± 1	nd	26.19
ProCAT-V1	78.1 ± 1	3.2 ± 1	7 ± 3	50 ± 1	0.09	15.62
ProCAT-V3	55 ± 2	6.5 ± 1	15 ± 3	48 ± 1	0.27	7.38
PCP-K47A	98 ± 9	3.8 ± 1	2 ± 1	98 ± 2	0.02	25.8
PCP-K47D	85 ± 8	5.8 ± 1	5 ± 1	92 ± 5	0.06	15.9

[a] nd, not detectable.

more ACP-like. At the same time, catalytic efficiency of Sfp with ProCAT-V3 is decreased to 50% of that with ProCAT.

A major difference between ACPs and PCs that became evident from sequence alignments can be found in residue 47 of PCP, which is the equivalent of residue 38 in ACP. In PCPs, this residue is usually His or Asp (6). In ACP, this position is almost exclusively occupied by positively charged amino acids such as Lys or Arg that form a hydrogen bond with R14 of AcpS (see Discussion). The fact that mutant ProCAT-V1, which contains the mutation K47D to make its PCP domain more ACP-like, was accepted as substrate by AcpS led to the construction of the PCP mutants PCP-K47D and PCP-K47A. Michaelis−Menten kinetics, determined by HPLC method A where the concentration of the CPs was varied from 1 to 100 μM, with these mutants as substrate for AcpS and Sfp yielded kinetic constants (Table 2) that are almost unchanged for Sfp compared to the wild-type PCP. AcpS, on the other hand, exhibits catalytic efficiencies that are reduced by factors of 30 and 90 compared to ACP and by factors of 10 and 30 compared to hPCP for PCP-K47D and PCP-K47A, respectively. Thus, a single mutation suffices to enable AcpS to recognize PCP in vitro. To address the question whether this would also hold true for a larger construct, the PCP domain in ProCAT was mutated in the same manner, which yielded mutants ProCAT-K47A and ProCAT-K47D. These proteins were qualitatively tested for interaction with AcpS with the priming assay method (Figure 5). The assay showed that AcpS can modify the PCP domain of both mutants even in the context of other domains.
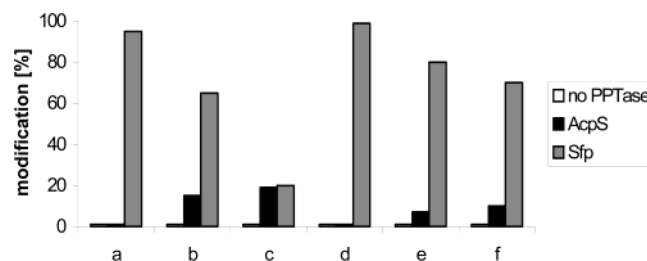

FIGURE 5: Posttranslational modification of the K47 mutants of TycC3-PCP and ProCAT by AcpS and Sfp in vitro. (a) Wild-type PCP (control); (b) PCP-K47A; (c) PCP-K47D; (d) wild-type ProCAT (control); (e) ProCAT-K47A; (f) ProCAT-K47D. CPs (1 μM) were incubated with 20 μM CoA, 200 nM [^{3}H]-CoA, and 10 mM MgCl$_2$ for 30 min at 37 °C. The wild-type proteins were modified by Sfp only, as expected, whereas all mutant proteins were also modified by AcpS.

Mutational Analysis of AcpS. From the findings described above, it became evident that the interaction of AcpS residues with residue 47 of PCP plays a major role for the substrate selectivity of this enzyme. The cocrystal structure of AcpS with ACP had shown that the equivalent residue in ACP, D38, is involved in the interaction with AcpS's residue R14. In addition, a superposition of AcpS and Sfp (27) led to a model where the K44 of the adjacent AcpS monomer is also involved in the interaction with D38 of ACP (see Discussion). This, however, was not seen in the cocrystal structure of AcpS with ACP because Parris et al. (8) have crystallized the K44A mutant of the enzyme (PDB code 1F80).

To answer the question whether mutations in AcpS would broaden the enzyme's substrate selectivity toward PCP, residues R14 and K44 were mutated. We first created the mutants AcpS-R14A and AcpS-K44A to show the involvement of these residues in the recognition of ACP. To make AcpS more Sfp-like, we have also constructed mutants AcpS-R14K and AcpS-K44D as well as the double mutant. All mutants were biochemically characterized by HPLC method B with ACP as the variable substrate. For this purpose, ACP was varied from 2 to 17 μM in nine steps and from 34 to 170 μM in six steps. This was necessary because AcpS usually exhibits two K_m values with ACP (19). Kinetic constants, which were determined through a Michaelis−Menten fit of the data sets, can be found in Table 3. A very prominent feature of all except mutant AcpS-R14K is that they have only one K_m for ACP. The replacement of Arg by Lys in mutant AcpS-R14K represents a fairly conservative change and does not seem to change AcpS's catalytic properties much. Both AcpS-K44A and AcpS-R14A exhibit catalytic efficiencies that are diminished by factors of almost 500 and 130, respectively, compared to wild type. This indicates that both residues play important roles in catalysis. Mutants AcpS-K44D and AcpS-R14K and the double mutant AcpS-K44D,R14K all show a definite change in K_m for ACP, which is comparable to the K_m Sfp exhibits for ACP. Catalytic efficiencies for high (20−200 μM) ACP concentrations, which are diminished by factors of 235, 22, and 43, respectively, for mutants AcpS-K44D, AcpS-R14K, and AcpS-K44D,R14K compared to AcpS, are also comparable to the efficiency of Sfp with high ACP concentrations. Surprisingly, AcpS-R14K has in fact a higher catalytic efficiency when low (2−17 μM) ACP concentrations are used than AcpS does under the same conditions.

Table 3: Kinetic Constants of AcpS Mutants and Sfp with ACP

| AcpS mutant	K_m (μM)	k_{cat} (min^{-1})	k_{cat}/K_m (min^{-1} μM^{-1})
Sfp (2−8 μM ACP)	1.4 ± 0.3	1.7 ± 0.1	1.2
Sfp (20−200 μM ACP)	38 ± 8	12.5 ± 1	0.3
AcpS (2−8 μM ACP)	0.2 ± 0.3	22 ± 2	129
AcpS (20−200 μM ACP)	68 ± 11	125 ± 9	1.8
R14A (1.9−235 μM ACP)	21.17 ± 3.03	21.42 ± 0.96	1.01
K44A (2−173 μM ACP)	120.52 ± 28.08	31.34 ± 4.04	0.26
R14K (2−34 μM ACP)	6.43 ± 1.92	96.47 ± 11.92	15.0
R14K (17.4−173 μM ACP)	25.77 ± 6.08	153.5 ± 10	5.96
K44D (2−173 μM ACP)	22.66 ± 5.43	12.54 ± 0.94	0.55
R14K, K44D (2−173 μM ACP)	29.41 ± 6.41	87.36 ± 6.40	2.97
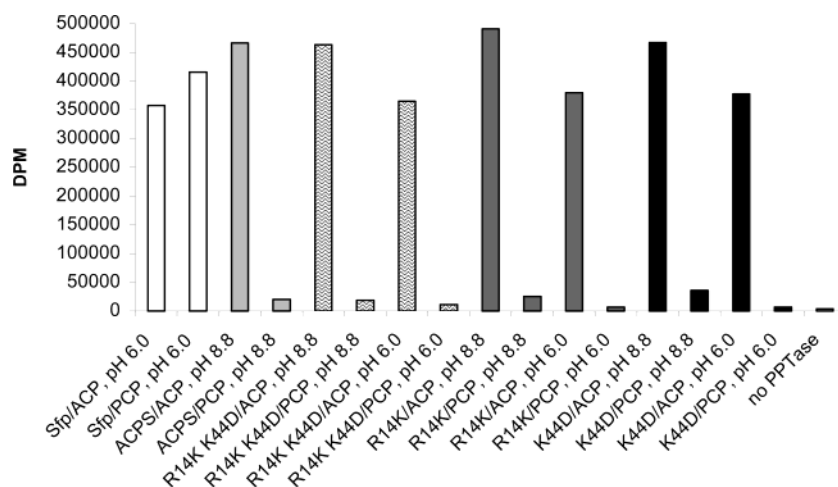
FIGURE 6: Substrate selectivity of the AcpS mutants. 500 nM PPTase were incubated with 50 μM CP, 12 mM MgCl$_2$, 20 μM CoA and 200 nM [^{3}H]CoA for 18 h at 37 °C. Shown are the DPM that were measured with the different PPTases at pH 8.8 or 6.0. ACP was modified by AcpS and PCP by Sfp, as expected, whereas the AcpS mutants were only capable of modifying ACP. With the exception of mutant K44D, which exhibits a slightly increased modification rate with PCP, none of the mutants significantly modified PCP under these conditions.

Because the catalytic efficiencies and K_m values for mutants AcpS-K44D, AcpS-R14K, and AcpS-K44D R14K were a lot like those of Sfp, we were encouraged to also test if PCP would be accepted as substrate by any of the mutants. For this purpose, all five AcpS mutants (1 μM) and Sfp (800 nM) as well as AcpS (1 μM) were individually incubated with ACP and with PCP (50 μM) in the presence of ^{3}H-labeled CoA for 18 h either at pH 8.8 (optimal pH of AcpS) or at pH 6.0 (optimal pH of Sfp). The result of this experiment can be seen in Figure 6. AcpS, Sfp, and each of the AcpS mutants modified ACP, as expected. None of the AcpS mutants, however, accepted PCP as substrate. As an exception, the amount of ACP modified by AcpS-K44D is slightly increased compared to AcpS. In addition, ACP was modified to a greater extent at pH 8.8 compared to pH 6.0 by all AcpS mutants, showing that the optimal pH for AcpS activity is unchanged. Interestingly, incubation of AcpS with PCP resulted in an amount of modification that is increased by a factor of 5.5 compared to reactions where the PPTase was omitted, indicating that the substrate discrimination of AcpS is not as strict as previously assumed.

Interaction of PCP Mutants with the Adenylation Domain of ProCAT. Interaction of the PCP mutants with the A domain was investigated by covalent loading of [^{14}C]-L-Pro to the 4′PP. Each ProCAT mutant (1 μM) or, for comparison, wild-type ProCAT was preincubated with 2 μM labeled amino acid, 20 μM CoA, and 25 nM recombinant *B. subtilis* AcpS or Sfp for 30 min at 37 °C. After preincubation, 5

mM ATP was added to the reaction mixtures and the amount of labeled protein was determined after an additional 5 min of incubation time. As can be seen in Figure 7, the ProCAT mutants K47A, K47D, V1, and V3 were modified in vivo to the holo form to 10%, 15%, 12%, and 70%, respectively, during expression by an *E. coli* PPTase, whereas wild-type ProCAT was only modified to about 1%. Additional incubation of these mutants in vitro with a PPTase shows that both AcpS and Sfp were able to modify ProCAT-K47A, -K47D, -V1, and -V3, resulting in an increase in the amount of loading catalyzed by the A domain. Wild-type ProCAT was not modified by AcpS, as expected. All ProCAT-LeuCAT-Te mutants were analyzed in the same manner and gave similar results (data not shown).

Communication of ProCAT Mutants with Other Modules. We have previously created a system composed of hTycA (PheATE) (where the PCP in TycA was replaced by the hPCP) and its natural protein partner TycB1 (ProCAT) that tested positive for production of the dipeptide D-Phe-L-Pro-diketopiperazine (DKP) (6). The hPCP was unable to communicate with the epimerization (E) domain of hTycA and was impaired in communication with TycB1's condensation (C) domain. This prompted us to investigate the ability of the ProCAT mutants created in this work to elongate amino acids in trans with their native partner TycA or hTycA as well as in cis with TycC6 (LeuCAT-Te).

We first incubated TycA with the ProCAT mutants or with the mutants of ProCAT-LeuCAT-Te for the production of the dipeptide D-Phe-L-Pro-DKP. The holoenzymes were
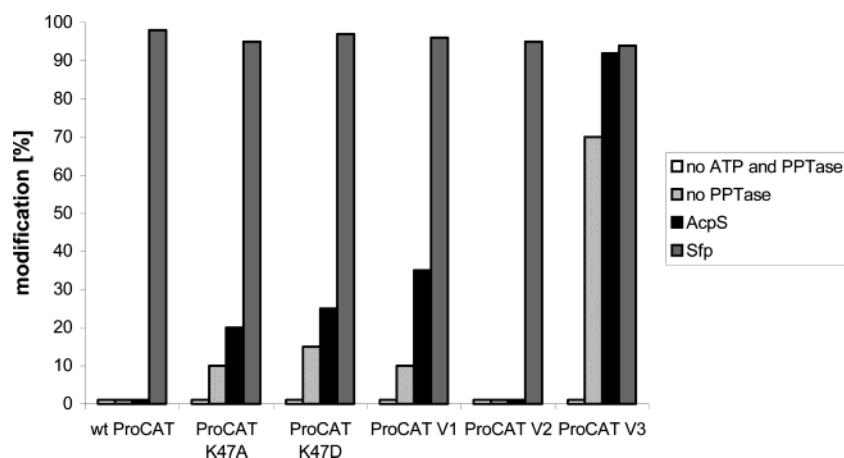
FIGURE 7: Posttranslational modification of ProCAT as well as its mutants by AcpS and Sfp and subsequent aminoacylation with [^{14}C]-L-Pro. ProCAT or its mutants (1 μM) were incubated with 2 μM [^{14}C]-L-Pro, 20 μM CoA, and 25 nM AcpS or Sfp for 30 min at 37° C. ATP (5 mM) was subsequently added to the reaction mixture, which was incubated for an additional 5 min at 37 °C. The assay revealed that the ProCAT mutants K47A, K47D, V1, and V3 were modified to 10%, 15%, 12%, and 70%, respectively, during expression. Wild-type ProCAT, on the other hand, was only modified to 1%. After in vitro incubation of the mutant proteins with a PPTase, aminoacylation was increased in the case of the mutants K47A, K47D, V1, and V3.

Table 4: FPL and DKP Production of TycA or hTycA in Combination with TycC6 Mutants[a]

	TycA (%)				hTycA (%)			
	−ATP, −PPTase	−ATP, +PPTase	AcpS	Sfp	−ATP, −PPTase	−ATP, +PPTase	AcpS	Sfp
ProCAT-Le uCAT-Te	0 (0)	0 (0)	0 (0)	100 (100)	0 (0)	0 (0)	0 (0)	85 (25)
ProCAT-V1-LeuCAT-Te	0 (0)	0 (0)	0 (0)	90 (85)	0 (0)	0 (7)	0 (30)	79 (27)
ProCAT-V2-LeuCAT-Te	0 (0)	0 (0)	0 (0)	95 (97)	0 (0)	0 (0)	0 (0)	80 (23)
ProCAT-V3-LeuCAT-Te	0 (0)	0 (0)	0 (0)	85 (79)	0 (0)	0 (15)	0 (23)	75 (22)

[a] FPL production is listed first; DKP production is listed second, in parentheses.

separately incubated with L-Phe and L-Pro, respectively, as well as ATP at 37 °C. The product D-Phe-L-Pro-DKP was identified and quantified by HPLC-ESI-MS [retention time 16.16 min, M$^+$ = 245.2 Da, calculated M$^+$ = 245 Da (*31*)]. As Table 3 shows, all ProCAT point mutants were capable of producing DKP in the presence of TycA. Mutants ProCAT-K47A, ProCAT-K47D, and ProCAT-V2 produce an amount of DKP that is at the level of wild-type ProCAT (97%, 98%, and 97% of wild type, respectively). ProCAT-V1 and ProCAT-V3, on the other hand, produce merely 85% and 79% DKP, respectively, compared with wild type. Incubation of TycA with the mutants ProCAT-V1-LeuCAT-V1−3 yields the exact same percentage of DKP production (Table 4). When hTycA was used in place of TycA, DKP production was observed with the in vivo modified proteins ProCAT-V1-LeuCAT-Te and ProCAT-V3-LeuCAT-Te in the absence of a PPTase at 7% and 15% of the wild-type level with TycA, respectively. Further in vitro modification of these proteins with AcpS raised production levels to 30% and 23%, respectively (Table 4). Wild-type ProCAT-LeuCAT-Te and the V2 mutant were only capable of DKP production after in vitro modification with Sfp. Production levels were low at 25% and 23%, respectively, for the wild type and the V2 mutant but confirmed earlier results (*6*).

Formation of the tripeptide product D-Phe-L-Pro-L-Leu (FPL) was used as an indicator for the functionality of a trimodular system comprising TycA or hTycA in combination with the ProCAT-LeuCAT-Te mutants. For this purpose, first the holoenzymes TycA and the ProCAT-LeuCAT-Te

mutants or wild type were incubated with L-Phe, L-Pro, L-Leu, and ATP in condensing buffer at 37 °C. As Table 3 shows, FPL production levels of TycA with the mutants were almost as high as for the wild type (90%, 95%, and 85%, respectively, for mutants ProCAT-LeuCAT-Te -V1−V3). Interestingly, incubation of the ProCAT-LeuCAT-Te mutants with hTycA leads to production of both DKP and FPL. Both products were identified and quantified by HPLC-ESI-MS. Analysis of the substance at 16.15 min yielded an M$^+$ of 245.2 Da, which corresponds to the calculated mass (245 Da) of D-Phe-L-Pro-DKP (*31*), while the product at 21.21 min had an M$^+$ of 376.3 Da, which is in agreement with the mass of D-Phe-L-Pro-L-Leu [M$^+$ = 376 Da (*29*)]. Whereas in vivo modification levels are too low for the production of FPL in the absence of a PPTase, synthesis of the tripeptide is observed (25%, 27%, 23%, and 22%, respectively, for wild type and mutants V1−3) after in vitro modification with Sfp. However, mutants ProCAT-LeuCAT-Te-V1 and -V3 did produce DKP even without further in vitro modification (7% and 15%, respectively, Table 4), and the level of production could be raised to 30% and 23%, respectively, after in vitro pantetheinylation with AcpS, while production of FPL was not observed. Thus, in this case, production of DKP and FLP can be controlled by selection of the appropriate PPTase.

DISCUSSION

The 4′-phosphopantetheinyl group is an essential cofactor of several multifunctional enzymes such as NRPSs and PKSs as well as of the multienzyme complex FAS. Therefore, the PPTases that posttranslationally transfer this moiety to the
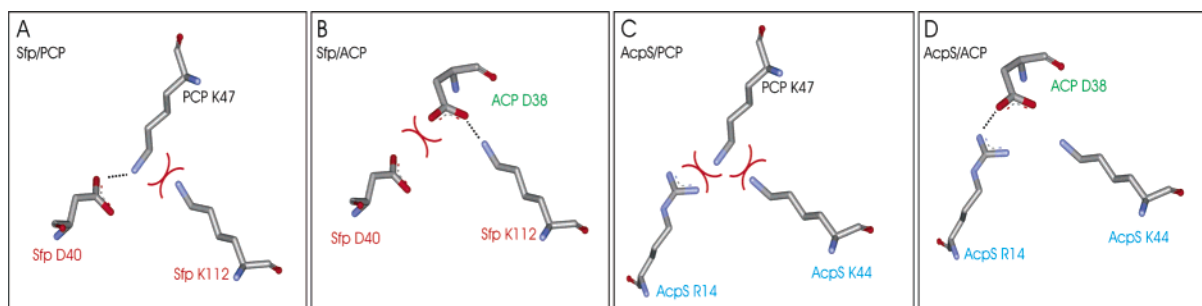
FIGURE 8: Postulated ACP and PCP binding sites of AcpS and Sfp. (A) Sfp uses residue D40 to interact with K47 of PCP, whereas (B) Sfp interacts with ACP's residue D38 via its K112. (C) AcpS cannot bind PCP because residues R14 and K44 repel PCP's K47, whereas (D) R14 is suitable to bind residue D38 of ACP.

CPs of these enzymes play an essential role in both primary and secondary metabolism. For this purpose, nature has evolved two different kinds of PPTases in prokaryotes, the AcpS type that accepts CPs of primary (FAS) metabolism and a promiscuous representative, the Sfp type, that modifies a wide variety of CPs. Crystal structures of both AcpS and Sfp have recently been solved. These structures revealed first of all that AcpS-type PPTases are enzymatically active homotrimers whereas Sfp is a pseudohomodimer composed of two halves that resemble the AcpS monomer (*27*). Thus, the Sfp type may be evolutionary related to the AcpS type.

A previous study has shown that a replacement of 14 amino acids in helix 2 of PCP with the corresponding amino acids of ACP enables AcpS to recognize the hybrid protein (*6*). In the present study, we have constructed three PCP mutants (V1−3) that enabled us to take a closer look at the individual residues involved in the CP−PPTase recognition. In contrast to wild-type PCP, mutants PCP-V1 and -V3 were modified in vivo by an endogenous *E. coli* PPTase. Further in vitro analysis confirmed that the catalytic efficiencies correlate with the number of mutations that make the protein more ACP-like. Mutant PCP-V2 is not recognized by AcpS, which indicates that residues 56 and 57 are not sufficient for recognition.

Analysis of the superfamily of CPs has revealed obvious divergences between PCPs and ACPs (*5, 6*). For instance, residue 47 of all types of PCPs is mostly occupied by positively charged amino acids such as Lys or Arg, rarely by Gln or Asn. The corresponding residue of ACP, 38, is exclusively occupied by Asp. The single mutants PCP-K47A and PCP-K47D confirmed the importance of this residue in the recognition of substrates by AcpS (Table 2). Analysis of the AcpS cocrystal structure revealed that residues R14 and K44 are within hydrogen-bond distance of D38 of ACP. The equivalent residues of the Sfp, as determined by superposition with the AcpS structure (*27*), are K112 and D40 that interact with K47 of PCP. On the basis of this analysis we propose a model for the CP binding pockets of AcpS and Sfp, which is depicted in Figure 8. In the case of Sfp, K47 of PCP and D38 of ACP engage in electrostatic interaction with residues D40 and K112 of Sfp, respectively (Figure 8A,B). The difference in charge between Asp and Lys confers flexibility on Sfp in the adaptation to various carrier proteins. However, K47 of PCP cannot interact electrostatically favorably with either R14 or K44 of AcpS (Figure 8C), whereas R14 is used to hydrogen-bond with D38 of ACP (Figure 8D). Mutation of the AcpS residues R14 and K44 to Ala confirms their involvement in CP

recognition. Also, comparison of the K_m values of these mutants reveals that K44 is more important than R14 for CP recognition, while partial compensation occurs because R14 can take over the function of K44 in the AcpS-K44A mutant and vice versa (Table 3). This hypothesis is supported by mutant AcpS-K44D. According to the model, the Asp residue should repel ACP, which is expressed in a catalytic efficiency that is reduced by a factor of 3 and a drop in k_{cat} by a factor of 10. The AcpS-K44D mutation does not lead to strict discrimination: the K_m and k_{cat} values are comparable to those that Sfp exhibits for ACP, possibly because the CP binding pocket of the AcpS-K44D mutant, just like that of Sfp, contains a positively (Arg) and a negatively (Asp) charged residue (Table 3). In addition, all AcpS mutants except AcpS-R14K exhibit only one K_m value for low and high CP concentrations. It seems that these AcpS mutants cannot carry out catalysis by the proposed, allosteric mechanism any longer (*19, 32*). The double mutant AcpS-R14K,-K44D imitates the K112/D40 situation found in Sfp. It was therefore expected that PCP's K47 is no longer electrostatically repelled. The experiment with labeled CoA, however, showed, that even after 18 h of incubation no increase in modification of TycC3−PCP compared to wild-type AcpS was achieved (Figure 7). Because the pH optima of both AcpS (8.8) and Sfp (6.0) were taken into account, it can be excluded that the optimum pH of any of the mutants has changed compared to wild type.

Sfp's CP recognition site is a flexible loop (*27*), whereas AcpS uses a rigid helix (Figure 3A) (*8*) for the interaction with ACP, which may also contribute to the strict discrimination among CP substrates by the enzyme. However, the structure of the CP may also play a role in the recognition process. Earlier investigations have pointed to a certain flexibility of ACPs (*11, 14*) that may enable the protein to interact with many different partners by adjusting its structure. Because PCPs are usually part of a larger polypeptide chain, a rigid structure would probably contribute to the directional synthesis along the NRPS template by restricting the PCP to interact solely with the domains of its own and the immediate downstream module.

Covalent loading of labeled L-Pro to the ProCAT mutants revealed that modification with the 4′PP in vivo corroborates our in vitro results, thus demonstrating that mutants PCP-K47A, -K47D, -V1, and -V3 are primed by endogenous *E. coli* AcpS during expression. The amount of loading by the A domain was increased after incubation of the mutants with either *B. subtilis* AcpS or Sfp, which confirmed earlier results that communication with the A domain is not altered by

mutations in helix 2 of the CP (6). To test if the mutants would still qualify for elongation, we have used both the mutants of ProCAT and ProCAT-LeuCAT-Te to produce D-Phe-L-Pro-DKP by interaction with TycA. Whereas mutants K47A, K47D, and V2 produce DKP at wild-type levels, V1 and V3 are slightly impaired in elongation (Table 4). This result indicates that residues 44, 50, 56, and 57 of PCP (numbering according to the excised TycC3−PCP) may play a role in communication with the C domain. DKP production was even lower when hTycA was used in place of TycA (Table 4), which points to a cumulative effect of the mutations in hTycA and ProCAT. Whereas all ProCAT-LeuCAT-Te mutants tested positive for the production of the tripeptide FPL with TycA, the mutations can be exploited for the selective production of DKP or FPL in combination with hTycA. Because in vivo pantetheinylation levels are too low for the production of FPL, in vitro modification with AcpS leads solely to increased production of DKP. The mutants were capable of FPL production only after modification with Sfp.

A single mutation in PCP or PCP domains of NRPS modules is sufficient to allow the constructs to be recognized in vivo and in vitro by AcpS, which demonstrates the close evolutionary relationship of the two classes of CPs. The AcpS- and Sfp-type PPTases are also thought to be evolutionarily related but differ significantly in their mode of recognition of CPs (27). Although we have identified residues involved in the AcpS−ACP and AcpS−PCP recognition, simple mutations did not suffice to produce an AcpS variant that modifies wild-type PCPs. Hence, diversification must have played a major role on the way from AcpS-type PPTases to the promiscuous Sfp-type PPTases of primary metabolism found in certain bacteria and in humans (25, 33).

ACKNOWLEDGMENT

REFERENCES

1. Schwarzer, D., Finking, R., and Marahiel, M. A. (2003) Nonribosomal peptides: from genes to products, *Nat. Prod. Rep. 20*, 275−287.
2. Cane, D. E., and Walsh, C. T. (1999) The parallel and convergent universes of polyketide synthases and nonribosomal peptide synthetases, *Chem. Biol. 6*, R319−325.
3. Hopwood, D. A. (1997) Genetic Contributions to Understanding Polyketide Synthases, *Chem. Rev. 97*, 2465−2497.
4. Joshi, A. K., Rangan, V. S., Witkowski, A., and Smith, S. (2003) Engineering of an active animal fatty acid synthase dimer with only one competent subunit, *Chem. Biol. 10*, 169−173.
5. Linne, U., Doekel, S., and Marahiel, M. A. (2001) Portability of Epimerization Domain and Role of Peptidyl Carrier Protein on Epimerization Activity in Nonribosomal Peptide Synthetases, *Biochemistry 40*, 15824−15834.
6. Mofid, M. R., Finking, R., and Marahiel, M. A. (2002) Recognition of hybrid peptidyl carrier proteins/acyl carrier proteins in nonribosomal peptide synthetase modules by the 4′-phosphopantetheinyl transferases AcpS and Sfp, *J. Biol. Chem. 277*, 17023−17031.
7. Holak, T. A., Kearsley, S. K., Kim, Y., and Prestegard, J. H. (1988) Three-dimensional structure of acyl carrier protein determined by NMR pseudoenergy and distance geometry calculations, *Biochemistry 27*, 6135−6142.
8. Parris, K. D., Lin, L., Tam, A., Mathew, R., Hixon, J., Stahl, M., Fritz, C. C., Seehra, J., and Somers, W. S. (2000) Crystal structures of substrate binding to *Bacillus subtilis* holo-(acyl carrier protein) synthase reveal a novel trimeric arrangement of molecules resulting in three active sites, *Struct. Fold Des. 8*, 883−895.
9. Weber, T., Baumgartner, R., Renner, C., Marahiel, M. A., and Holak, T. A. (2000) Solution structure of PCP, a prototype for the peptidyl carrier protein domains of modular peptide synthetases, *Struct. Fold Des. 8*, 407−418.
10. Xu, G. Y., Tam, A., Lin, L., Hixon, J., Fritz, C. C., and Powers, R. (2001) Solution structure of *B. subtilis* acyl carrier protein, *Structure (Cambridge) 9*, 277−287.
11. Wong, H. C., Liu, G., Zhang, Y.-M., Rock, C. O., and Zheng, J. (2002) The solution structure of acyl carrier protein from *Mycobacterium tuberculosis*, *J. Biol. Chem. 277*, 15874−15880.
12. Findlow, S. C., Winsor, C., Simpson, T. J., Crosby, J., and Crump, M. P. (2003) Solution structure and dynamics of wxytetracycline polyketide synthase acyl carrier protein from *Streptomyces rimosus*, *Biochemistry 42*, 8423−8433.
13. Flaman, A. S., Chen, J. M., Van Iderstine, S. C., and Byers, D. M. (2001) Site-directed mutagenesis of Acyl carrier protein reveals amino acid residues involved in ACP structure and Acyl-ACP synthetase activity, *J. Biol. Chem. 276*, 35934−35939.
14. Andrec, M., Hill, R. B., and Prestgard, J. H. (1995) Amide exchange rates in *Escherichia coli* acyl carrier protein: correlation with protein structure and dynamics, *Protein Sci. 4*, 983−993.
15. Zhang, Y. M., Rao, M. S., Heath, R. J., Price, A. C., Olson, A. J., Rock, C. O., and White, S. W. (2001) Identification and analysis of the acyl carrier protein (ACP) docking site on beta-ketoacyl-ACP synthase III, *J. Biol. Chem. 276*, 8231−8238.
16. Lambalot, R. H., Gehring, A. M., Flugel, R. S., Zuber, P., LaCelle, M., Marahiel, M. A., Reid, R., Khosla, C., and Walsh, C. T. (1996) A new enzyme superfamily—the phosphopantetheinyl transferases, *Chem. Biol. 3*, 923−936.
17. Flugel, R. S., Hwangbo, Y., Lambalot, R. H., Cronan, J. E., Jr., and Walsh, C. T. (2000) Holo-(acyl carrier protein) synthase and phosphopantetheinyl transfer in *Escherichia coli*, *J. Biol. Chem. 275*, 959−968.
18. Chirgadze, N. Y., Briggs, S. L., McAllister, K. A., Fischl, A. S., and Zhao, G. (2000) Crystal structure of *Streptococcus pneumoniae* acyl carrier protein synthase: an essential enzyme in bacterial fatty acid biosynthesis, *EMBO J. 19*, 5281−5287.
19. Mootz, H. D., Finking, R., and Marahiel, M. A. (2001) 4′-Phosphopantetheine Transfer in Primary and Secondary Metabolism of *Bacillus subtilis*, *J. Biol. Chem. 276*, 37289−37298.
20. Sanchez, C., Du, L., Edwards, D. J., Toney, M. D., and Shen, B. (2001) Cloning and characterization of a phosphopantetheinyl transferase from *Streptomyces verticillus* ATCC15003, the producer of the hybrid peptide—polyketide antitumor drug bleomycin, *Chem. Biol. 8*, 725−738.
21. Mofid, M. R., Marahiel, M. A., Ficner, R., and Reuter, K. (1999) Crystallization and preliminary crystallographic studies of Sfp: a phosphopantetheinyl transferase of modular peptide synthetases, *Acta Crystallogr. D: Biol. Crystallogr. 55*, 1098−1100.
22. Reuter, K., Mofid, M. R., Marahiel, M. A., and Ficner, R. (1999) Crystal structure of the surfactin synthetase-activating enzyme Sfp: a prototype of the 4′-phosphopantetheinyl transferase superfamily, *EMBO J. 18*, 6823−6831.
23. Gehring, A. M., Lambalot, R. H., Vogel, K. W., Drueckhammer, D. G., and Walsh, C. T. (1997) Ability of *Streptomyces* spp. acyl carrier proteins and coenzyme A analogues to serve as substrates in vitro for *E. coli* holo-ACP synthase, *Chem. Biol. 4*, 17−24.
24. Quadri, L. E., Weinreb, P. H., Lei, M., Nakano, M. M., Zuber, P., and Walsh, C. T. (1998) Characterization of Sfp, a *Bacillus subtilis* phosphopantetheinyl transferase for peptidyl carrier protein domains in peptide synthetases, *Biochemistry 37*, 1585−1595.
25. Finking, R., Solsbacher, J., Konz, D., Schobert, M., Schäfer, A., Jahn, D., and Marahiel, M. A. (2002) Characterization of a new type of phosphopantetheinyl transferase for fatty acid and siderophore metabolism in *Pseudomonas aeruginosa*, *J. Biol. Chem. 277*, 50293−50302.
26. Keszenman-Pereyra, D., Lawrence, S., Twfieg, M. E., Price, J., and Turner, G. (2003) The *npgA/cfwA* gene encodes a putative 4′-phosphopantetheinyl transferase which is essential for penicillin biosynthesis in *Aspergillus nidulans*, *Curr. Genet. 43*, 186−190.
27. Mofid, M. R., Finking, R., and Marahiel, M. A. (2004) Structure-based mutational analysis of the 4′-phosphopantetheinyl transferases Sfp from *Bacillus subtilis*: carrier protein recognition and reaction mechanism, *Biochemistry 43*, 4128−4136.

28. Sambrook, J., Fritsch, E. F., and Maniatis, T. (1989) *Molecular Cloning: A Laboratory Manual*, Cold Spring Harbor Laboratory Press, Cold Spring Harbor, NY.

29. Mootz, H. D., Schwarzer, D., and Marahiel, M. A. (2000) Construction of hybrid peptide synthetases by module and domain fusions, *Proc. Natl. Acad. Sci. U.S.A. 97*, 5848−5853.

30. Linne, U., and Marahiel, M. A. (2000) Control of directionality in nonribosomal peptide synthesis: role of the condensation domain in preventing misinitiation and timing of epimerization, *Biochemistry 39*, 10439−10447.

31. Stachelhaus, T., Mootz, H. D., Bergendahl, V., and Marahiel, M. A. (1998) Peptide bond formation in nonribosomal peptide biosynthesis. Catalytic role of the condensation domain, *J. Biol. Chem. 273*, 22773−22781.

32. McAllister, K. A., Peery, R. B., Meier, T. I., Fischl, A. S., and Zhao, G. (2000) Biochemical and molecular analyses of the *Streptococcus pneumoniae* acyl carrier protein synthase, an enzyme essential for fatty acid biosynthesis, *J. Biol. Chem. 275*, 30864−30872.

33. Joshi, A. K., Zhang, L., Rangan, V. S., and Smith, S. (2003) Cloning, expression and characterization of a human 4′-phospho-pantetheinyl transferase with broad substrate specificity, *J. Biol. Chem. 278*, 33142−33149.